Domain Formation in Phosphatidylinositol Monophosphate/Phosphatidylcholine Mixed Vesicles

Duane A. Redfern and Arne Gericke
Chemistry Department, Kent State University, Kent, Ohio

ABSTRACT Phosphoinositides have been shown to control membrane trafficking events by targeting proteins to specific cellular sites, which requires a tight regulation of phosphoinositide generation and turnover as well as a high degree of compartmentalization. To shed light on the processes that lead to the formation of phosphoinositide-enriched microdomains, phosphatidylcholine/phosphatidylinositol monophosphate (phosphatidylinositol-3-phosphate (PI-3P), -4-phosphate (PI-4P), or -5-phosphate (PI-5P)) mixed vesicles were investigated by calorimetric (DSC) Fourier transform infrared spectroscopic (FTIR), and fluorescence resonance energy transfer (FRET) measurements. The experiments furnished results consistent with a pH-dependent formation of phosphatidylinositol monophosphate-enriched microdomains. The domain formation was most pronounced between pH ≈7 and ≈9.5, whereas slightly acidic pH values (pH 4) resulted in the disintegration of the domains. This pH-dependent phosphatidylcholine/phosphatidylinositol monophosphate demixing was observed for the gel phase (FTIR experiments) as well as for the fluid lipid phase (FRET measurements). The observed microdomains are presumably stabilized by hydroxyl/hydroxyl as well as hydroxyl/phosphomonoester and phosphodiester interactions. While the pH dependence of the mutual phosphatidylinositol monophosphate interaction was largely the same for all investigated phosphatidylinositol monophosphates, it turned out that the relative stability of phosphatidylinositol monophosphate-enriched microdomains (pH 7–9.5) was governed by the position of the phosphomonoester group at the inositol ring (PI-4P > PI-5P > PI-3P). Demixing was also observed for phosphatidylcholine/phosphatidylinositol mixed vesicles; however, in this case the microdomain formation was only slightly affected by pH changes.

INTRODUCTION

Phosphoinositides (Fig. 1) have been shown to mediate a large variety of important physiological functions by affecting the activity and/or localization of membrane-associated proteins (Payrastre et al., 2001; Simonsen et al., 2001). The versatile inositol ring can be modified at several positions and a broad range of protein motifs bind with great specificity to the different phosphoinositides (Lemmon, 2003). The spatiotemporal control of protein function requires a precise regulation of phosphoinositide generation and turnover, which is facilitated by various kinases and phosphatases (Kanaho and Suzuki, 2002; Vanhaesebroeck et al., 2001), as well as a high degree of compartmentalization. Depending on the position of the phosphomonoester group at the inositol ring, phosphatidylinositol monophosphates have been shown to accumulate in specific cellular compartments. For example, phosphatidylinositol-3-phosphate (PI-3P) is an integral part of the endocytic pathway and is found to be highly enriched in early endosomes and intraluminal vesicles of multivesicular endosomes, while it is undetectable in plasma and Golgi membranes (Stenmark and Gillooly, 2001). In turn, phosphatidylinositol-4-phosphate (PI-4P) has been shown to be concentrated in Golgi membranes (Wang et al., 2003) and phosphatidylinositol-5-phosphate (PI-5P) is involved in plasma membrane trafficking events (Carricaburu et al., 2003; Padron et al., 2003). In addition to the cell compartment specific accumulation of phosphatidylinositol monophosphates, it has been suggested that many of the observed physiological functions require selective enrichment of phosphatidylinositol monophosphates in microdomains.

Recent studies reported the raft-dependent (Bodin et al., 2001; Caroni, 2001; Hill et al., 2002; Rozelle et al., 2000; Zhuang et al., 2002) and raft-independent (Botelho et al., 2000; Marshall et al., 2001; Miaczynska and Zerial, 2002) accumulation of phosphoinositides in defined membrane regions in vivo; however, the mechanisms that lead to the formation of phosphoinositide-enriched microdomains are elusive. The site-specific recruitment of phosphoinositide kinases (e.g., the targeting of type III PI 3-kinase by Rab5 to certain regions of the early endosome) and the resulting localized production of distinct phosphoinositides has been offered as a possible explanation for the formation of such microdomains (Miaczynska and Zerial, 2002). While these processes are certainly a contributing factor, they alone cannot explain local phosphoinositide enrichment, because diffusion away from the synthesis site will most likely limit the accumulation (McLaughlin et al., 2002). It has been shown that protein motifs rich in basic residues (e.g., MARCKS effector domain) induce phosphatidylinositol-4,5-bisphosphate sequestration by nonspecific electrostatic interactions (Wanaski et al., 2003; Wang et al., 2002; Zhang et al., 2003) and it has been suggested that such mechanisms play a broader role in the local accumulation of phosphoinositides (McLaughlin et al., 2002). On the other hand, the formation of phosphoinositide-enriched microdomains is likely to depend on several factors and in the light of the rich

Submitted October 27, 2003, and accepted for publication January 23, 2004.
Address reprint requests to Arne Gericke, E-mail: agericke@kent.edu.

0006-3495/04/05/2980/13 $2.00

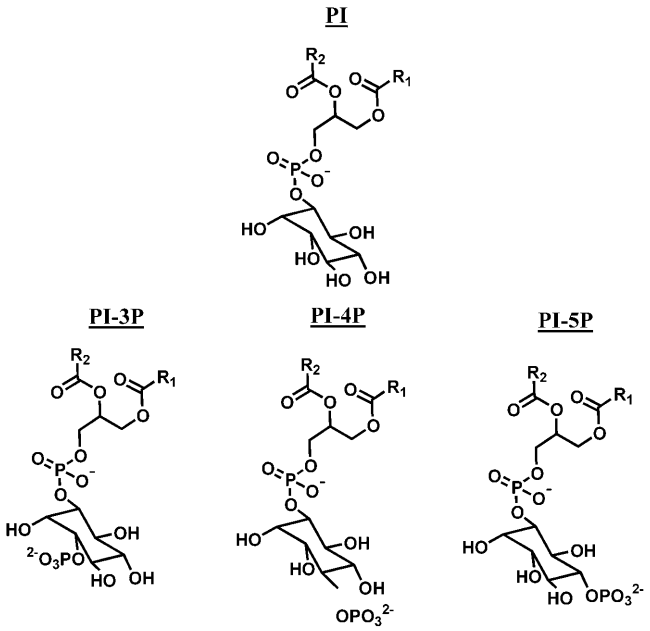

FIGURE 1 Chemical structures of phosphatidylinositol (*PI*), phosphatidylinositol-3-phosphate (*PI-3P*), -4-phosphate (*PI-4P*), and -5-phosphate (*PI-5P*).

phosphoinositide headgroup functionality it is conceivable that mutual interaction via hydrogen bond formation is an essential element for the formation of such domains.

Hydrogen bond formation between lipid headgroups has generally been identified as a source of lipid phase stabilization (Eibl, 1983). For example, the pH-dependent analysis of dipalmitoylphosphatidic acid (DPPA) phase behavior revealed increased gel-phase stability (higher main phase transition temperature) between the pK_{a1} and pK_{a2} of the phosphomonoester group (Eibl, 1983). This strong mutual phosphatidic acid (PA) interaction was also evident in calorimetric studies of mixed phosphatidylcholine (PC)/PA vesicles, which showed fluid/fluid immiscibility at pH 4 (Garidel et al., 1997a). The observed pH dependence of the mutual phosphatidic acid interaction was attributed to the fact that the presence of hydrogen-donating and hydrogen-accepting groups is required for the formation of a hydrogen bond network. Although this is fulfilled for a partially dissociated phosphomonoester group ($pKa_1 < pH < pKa_2$), this requirement is not satisfied for the fully protonated or deprotonated state. In the case of phosphoinositides, it is far more challenging to predict the mutual interaction because three types of functional groups (phosphodiester, phosphomonoester, and hydroxyl groups) can potentially participate in hydrogen bond formation. Furthermore, the number and position of the phosphomonoester groups at the inositol ring is likely to impact the mutual phosphoinositide interaction.

This study is concerned with the physicochemical characterization of phosphatidylinositol (PI) and phosphatidylinositol monophosphates, namely phosphatidylinositol-3-phosphate, -4-phosphate, and -5-phosphate. The experiments are designed to explore the pH dependence of the mutual phosphoinositide interaction and to highlight the importance of the position of the phosphomonoester group at the inositol ring for such interaction. Differential scanning calorimetry (DSC) and temperature-dependent infrared transmission spectroscopy are being used to study the pH-dependent mixing behavior of phosphatidylcholine and phosphatidylinositol monophosphate (PI-xP) multilamellar vesicles. The measurements not only highlight the gel-phase miscibility of the two lipid components but also provide information about the relative stability of phosphatidylinositol monophosphate-enriched domains. The results of these experiments are indicative of a pH-dependent PC/PI-xP gel-phase immiscibility and the question arises whether a similar immiscibility can also be found in fluid PC/PI-xP phases. To address this issue, a novel fluorescence resonance energy transfer (FRET) protocol was developed, which enables the pH-dependent analysis of PC/PI-xP fluid/fluid immiscibility in unilamellar vesicles. These FRET measurements furnished results, which are consistent with the formation of fluid PI-xP-enriched microdomains for pH ≈7–9, whereas a lowering of the pH results in an increased PC/PI-xP mixing.

MATERIALS AND METHODS

Materials

Dipalmitoylphosphatidylinositol (DPPI) was obtained from Matreya (Pleasant Gap, PA) and was used as received (98%+ purity). Dipalmitoylphosphatidylinositol-3-phosphate (DPPI-3P), -4-phosphate (DPPI-4P), and -5-phosphate (DPPI-5P) were obtained from Cayman Chemical (Ann Arbor, MI) and were also used as received (98%+ purity). For comparison, several experiments were reproduced with the respective phosphoinositides obtained from Matreya (98%+ purity), Echelon (Salt Lake City, UT; >95% purity) or A.G. Scientific (San Diego, CA; 99% purity). The integrity of the samples was confirmed by thin layer chromatography. The results obtained for samples from all four vendors were in general agreement. Dipalmitoylphosphatidylcholine (DPPC), 1-palmitoyl-2-oleoylphosphatidylcholine (POPC), brain phosphatidylinositol-4-phosphate, and acyl chain perdeuterated dipalmitoylphosphatidylcholine-d_{62} (DPPC-d_{62}) were obtained from Avanti Polar Lipids (Alabaster, AL) and were used as received (the purity of the synthetic lipids was 99%). Fluorescently labeled D(+)-*sn*-1-*O*-[1-[6′-[6-[((4-(4,4-difluoro-5-(2-thienyl)-4-bora-3a,4a-diaza-*s*-indacene-3-yl) phenoxy) acetyl) amino]hexanoyl]amino]hexanoyl]-2-hexanoylglyceryl D-*myo*-phosphatidylinositol 3-phosphate (BODIPY-PI-3P; excitation = 589 nm; emission = 617 nm) as well as the corresponding BODIPY-PI-4P and -PI-5P were obtained from Molecular Probes (Eugene, OR; purity >95%). PC-BODIPY (excitation = 581 nm; emission = 591 nm) was obtained from the same source. Chain-labeled 1-palmitoyl-2-[12-[(7-nitro-2-1,3-benzoxadiazol-4-yl)amino]dodecanoyl]-*sn*-glycero-3-phosphocholine (NBD-PC, excitation = 460 nm; emission = 534 nm) as well as NBD-PA and NBD-phosphatidylglycerol (PG) were obtained from Avanti Polar Lipids (Alabaster, Al). All buffers (HEPES, MES, CHES), as well as EDTA and NaCl, were of enzyme grade purity (Fisher Scientific, Chicago, IL). Buffers had the general composition 100 mM NaCl, 10 mM buffer, 0.1 mM EDTA, and were adjusted to the appropriate pH value by using aqueous HCl or NaOH, respectively. The buffers were used as follows: pH 9.5 CHES, pH 8.5 and 7.4 HEPES, and pH 6.5 and 5.5 MES. Chloroform and methanol, which were used to prepare lipid stock solutions, were ACS grade, whereas the water used for buffer preparation was HPLC grade (all Fisher Scientific, Chicago, IL).

Sample preparation

Lipids were stored in chloroform/methanol (2:1) stock solutions. Mixed multilamellar vesicles were prepared by drying appropriate amounts of the stock solutions in a stream of dry nitrogen. To avoid lipid demixing due to solubility differences among the components of the lipid mixture (which has been shown in some instances to affect the mixing properties in the later formed vesicles), this drying process was carried out as quickly as possible at slightly elevated temperatures (≈50°C). Subsequently, the samples were kept overnight in high vacuum at 45°C. The lipid mixtures were resuspended in the appropriate buffer solution, heated for 5–10 min at ≈50°C and vortexed for 60 s. This procedure was repeated two more times. For the DSC and infrared (IR) measurements these lipid suspensions were used for the measurement. The final total lipid concentrations were 0.3 mM for the DSC experiments and 40.6 mM (lipid/water ratio 1:25 w/w) for the FTIR measurements. For the fluorescence measurements, unilamellar vesicles were obtained by extruding the multilamellar vesicles at ≈60°C through a 100-nm pore size membrane (Avestin, Ottawa, ON). The quality of the extrusion was checked regularly by Dynamic Light Scattering (HPPS, Malvern Instruments, Southborough, MA). Typically, a narrow intensity distribution centered at 110- to 130-nm vesicle diameter was obtained. The lipid concentration used for the fluorescence experiments was identical to the DSC measurement concentrations, i.e., 0.3 mM.

Differential scanning calorimetry

DSC measurements of mixed multilamellar vesicles were carried out using a Microcal VP-DSC (Northampton, MA). The scan rate was 1.0°C/min and the total lipid concentration was 0.3 mM. A total of four heating/cooling cycles (4–90°C) were recorded and the third heating scan (fifth scan overall) was usually found to be representative.

Fourier transform infrared (FTIR) transmission spectroscopy

FTIR experiments were carried out with a Bruker Equinox Spectrometer (Billerica, MA) equipped with a broad band MCT detector. Interferograms were collected at 4 cm^{-1} resolution (1000 scans), apodized with a Blackman-Harris function, and Fourier transformed with two levels of zero filling to yield spectra encoded at 1 cm^{-1} intervals. Lipid samples (40.6 mM) were sandwiched between two BaF_2 windows (25 μm poly(tetrafluoroethylene) spacer) and placed in a Wilmad (Buena, NJ) temperature-controlled liquid cell holder. The sample temperature was monitored by using a thermocouple attached to an Omega (Stamford, CT) DP 116 thermometer (0.1°C relative accuracy). The sample temperature was adjusted by using a computer-controlled thermostated waterbath. The temperature-dependent acquisition of IR spectra between 4°C and 90°C took ≈30 h. Before and after completion of the IR experiment, the samples were checked for proper hydration by visual inspection and by monitoring the H_2O stretching band intensities. The spectra were processed by using the software supplied by the instrument manufacturer. The positions of the methylene stretching vibration bands were determined by calculating the second derivative followed by a center-of-mass peak pick algorithm. This typically results in a peak position accuracy of ± 0.1 cm^{-1}.

Fluorescence resonance energy transfer measurements

Fluorescence measurements were carried out using a Varian Eclipse fluorescence spectrometer (Walnut Creek, CA), equipped with a temperature controlled sample holder. Unilamellar mixed vesicles (0.288 mM total lipid, 85% PC/15% PI-xP) were made as described above and subsequently, aqueous buffer dispersions of the fluorescently labeled lipids were added to the preformed unilamellar vesicles. The samples were kept for at least 1 h at a temperature above the melting transition of the respective lipid mixtures (i.e., 70°C for saturated lipids, 20°C for unsaturated lipids). The insertion of the fluorescent lipids into the outer leaflet of the bilayer was monitored based upon the NBD-PC emission intensity (the NBD dye is nonfluorescent in an aqueous medium), which reached a steady state ≈60 min after the addition of the labeled lipids. The concentration of the respective NBD lipid was 0.6 mol % of the total lipid concentration, while the concentration of the BODIPY lipid was 0.72 mol %. These concentrations were determined to be optimal for a minimal transfer in the demixed state and a maximum resonance energy transfer in the mixed lipid state. The BODIPY-TR fluorophore (excitation = 589 nm; emission = 617 nm) used for this investigation is not the best FRET partner for the NBD fluorophore (excitation = 460 nm; emission = 534 nm). At first glance, BODIPY-TMR (excitation, 542 nm; emission 574 nm) appears to be a better partner for NBD because of the more favorable position of the absorption band. However, a closer inspection of the BODIPY-TMR absorption spectrum revealed a significant direct excitation of the BODIPY fluorophore for an excitation wavelength between 440 and 460 nm. In contrast, BODIPY-TR shows almost no direct excitation at this wavelength. For all FRET experiments an excitation wavelength of 440 nm was utilized. The labeled unilamellar vesicles were titrated with 0.1 N HCl from a high to a low pH value. After each titration step, samples were allowed to equilibrate for at least 6 min (longer waiting times did not furnish deviating results). The observed mixing properties of the respective lipid mixture were completely reversible, i.e., adjustment of the pH back to ≈10 at the end of the experiment resulted in similar resonance energy transfer ratios as at the beginning of the titration. The integrity of the vesicles was checked by Dynamic Light Scattering after completion of the titrations and no vesicle fusion or decomposition was detectable.

RESULTS

Differential scanning calorimetry

In Fig. 2, the DSC thermograms of pure DPPC and DPPI multilamellar vesicles are compared to the respective result of their 1:1 mixture. The DPPI thermogram shows a small transition peak at 38.5°C, while the main phase transition is

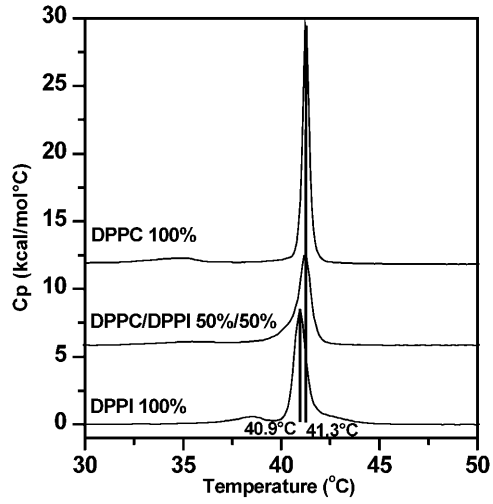

FIGURE 2 DSC thermograms of DPPC, DPPI, and DPPC/DPPI (1:1) multilamellar vesicles (0.3 mM total lipid concentration, third heating scan, heating rate = 1°C/min, pH 7.4, 100 mM NaCl, 10 mM HEPES, 0.1 mM EDTA).

located at 40.9°C. The enthalpy associated with this transition was found to be 7.9 ± 0.15 kcal/mol. The DPPI phase transition temperature and enthalpy were confirmed with samples from a different supplier (see Materials and Methods).

In comparison to DPPC, the DPPI main phase transition is shifted only slightly to lower temperature, but the increased width of the transition peak indicates a less cooperative behavior. In the case of DPPC, the small peak at 34.8°C is associated with a so-called pretransition from a gel to a ripple phase (Heimburg, 2000) and it is tempting to speculate that the small peak observed for DPPI at 38.5°C indicates a similar transition. For the 1:1 DPPC/DPPI mixture, the main phase transition (T_m) is found close to the T_m of DPPC, but the pretransition peak is abolished (which is typical for mixtures) and the cooperativity of the phase transition is reduced. Due to the similar DPPC and DPPI phase transition temperatures, it is not possible to judge based upon the DSC experiments whether or not lipid demixing occurs. The similar thermotropic behavior of DPPI and DPPC multilamellar vesicles generally indicates that the steric demand of the inositol ring resembles the spatial requirements of the phosphocholine headgroup.

The results obtained for DPPI are markedly different from those reported by Mansour et al. (2001), who found a surprisingly low T_m of −24.9°C for pure DPPI vesicles (similar to the T_m value they reported for Soy-PI, which is rich in unsaturated fatty acids). In contrast, Hanbro et al. (1992) reported for DMPI vesicles a gel/liquid-crystalline phase transition temperature of 19–21°C (enthalpy 5.8 ± 0.45 kcal/mol). An extension of the acyl chains from C_{14} to C_{16} typically gives rise to a gel/liquid-crystalline phase transition temperature increase of ≈15–20°C (Koynova and Caffrey, 1998), which implies that the phase transition temperature obtained by Hansbro et al. for DMPI (19–21°C) fits well the corresponding DPPI phase transition temperature (40.9°C) reported in this article.

Phosphoinositides usually form in aqueous solution—depending on pH and salt concentration—micellar or nonlamellar phases (Takizawa et al., 1998). Therefore, single-component phosphatidylinositol monophosphate systems are not suitable as models for biological membranes and instead phosphoinositide/lipid mixtures have to be used. We have investigated the thermotropic behavior of mixed DPPC/DPPI-xP (85:15) multilamellar vesicles for pH values between 5.5 and 9.5 (Fig. 3). For pH 5.5, the main phase transition temperature for all three investigated phosphoinositides was at or slightly above the respective phase transition temperature of pure DPPC. For the DPPI-3P- and DPPI-4P-containing mixtures a pretransition peak is discernable and the phase transition appears to be quite cooperative (narrow phase transition peak), while the phase transition was found to be less cooperative and the pretransition peak was abolished in the presence of DPPI-5P. In the case of DPPI-3P-containing mixtures, an increase of the pH value results in a gradual shift of the main phase transition temperature from 41.6°C (pH 5.5) to 40.5°C (pH 9.5). For all pH values, the main phase transition peak is quite narrow and a pretransition peak is clearly visible; however, upon increasing the pH value the position of the pretransition shifts from 34.5°C to 29.6°C. In the case of the DPPI-4P- and DPPI-5P-containing mixtures, the phase transitions are less cooperative and the pretransition peak is absent at intermediate pH levels. The peak width reaches a maximum at pH 8.5 (in the presence of DPPI-5P a shoulder is found), whereas the corresponding phase transition temperature is at a minimum (40.1–40.2°C in both cases). A further increase of the pH results in a reduced width of the main phase transition peak and a reappearance of the pretransition peak. Generally, all DSC experiments showed a good reversibility, i.e., repeated heating scans matched very well and only a small hysteresis (difference of the T_m values for heating and cooling scans) is found (not shown). The use of slower scan rates (0.25°C/min) did not alter the results.

Infrared spectroscopy

Lipid phase behavior can be studied with FTIR spectroscopy by monitoring the position of the methylene stretching vibration bands, which have been shown to shift to higher wavenumbers as the lipid acyl chains become more disordered (McElhaney and Lewis, 1995; Mendelsohn and Snyder, 1996). In binary mixtures, the acyl chain order of the individual lipids can be analyzed independently by using an acyl chain deuterated lipid as one of the two components (Mendelsohn and Moore, 1998), i.e., the acyl chain order of the deuterated component can be analyzed based upon the antisymmetric CD_2 stretching vibration band ($\nu_a(CD_2)$), whereas the symmetric CH_2 stretching band ($\nu_s(CH_2)$) is used to monitor the acyl chain order of the nondeuterated lipid. As a result, the extent of lipid demixing (domain formation) can be analyzed by comparing the temperature-dependent behavior of the $\nu_a(CD_2)$ and the $\nu_s(CH_2)$ bands. For the purpose of this study, we used acyl chain deuterated DPPC-d_{62} as the deuterated component, which exhibits due to the isotopic labeling a slightly lower phase transition temperature than its nondeuterated analog (36.6°C instead of 41.3°C).

Fig. 4 shows the $\nu_a(CD_2)$ and $\nu_s(CH_2)$ band frequencies of DPPC-d_{62}/DPPI-xP (85:15) mixed multilamellar vesicles as a function of temperature. For all three DPPI-xP isomers a complex, pH-dependent phase behavior is observed. Concurrent with the DPPC-d_{62} main phase transition, the DPPI-xP components show a transition over a quite narrow temperature range, which is followed by a much broader second transition. The relative magnitude of the two DPPI-xP phase transitions is pH-dependent and varies among the different DPPI-xP isomers. For all three DPPI-xP isomers, the broad high-temperature transition is most pronounced for pH 7.4 and 8.5 and is almost vanished at pH 5.5. The

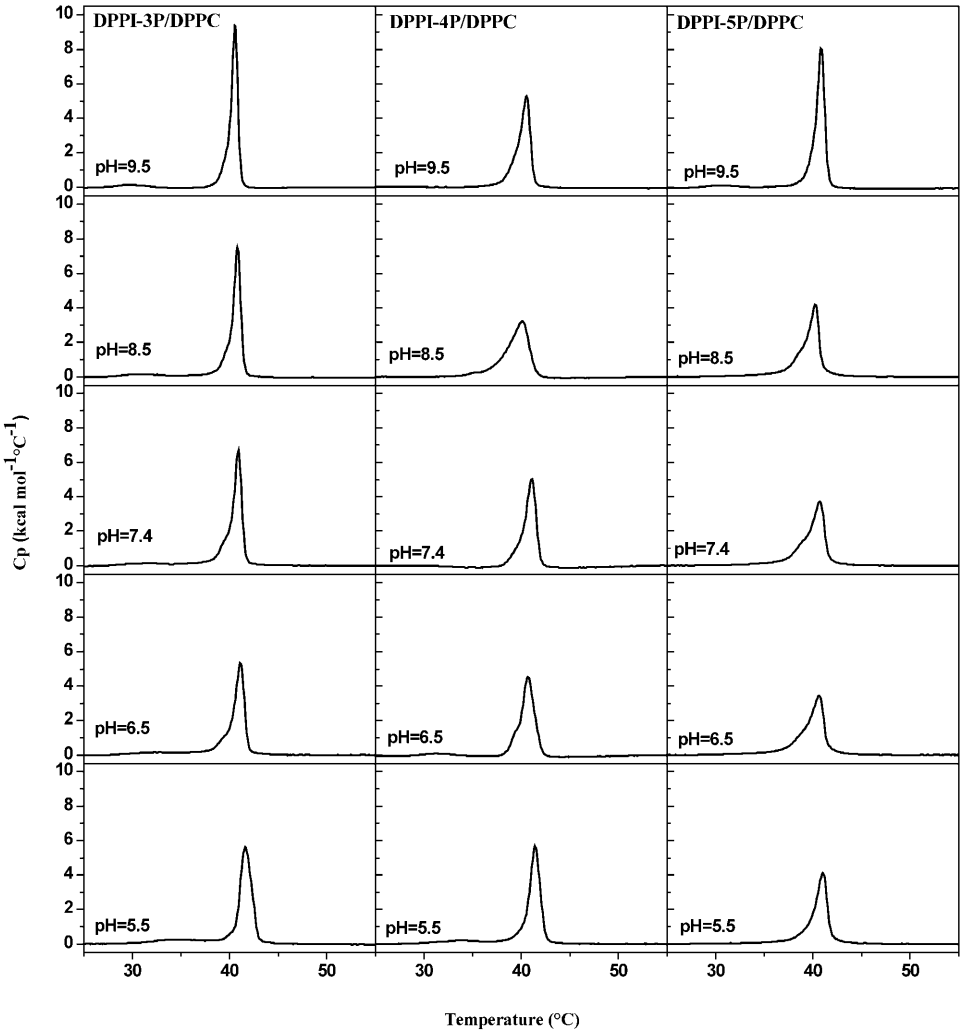

FIGURE 3 DSC thermograms of DPPC/DPPI-xP (85:15) mixed multilamellar vesicles as a function of pH value (0.3 mM total lipid concentration, third heating scan, heating rate = 1°C/min, 100 mM NaCl, 10 mM buffer, 0.1 mM EDTA, see Materials).

comparison of the different DPPI-xP isomers reveals that the second transition is most prominent for DPPI-4P, where the second transition is even reflected in the data points for the DPPC-d_{62} component. The temperature ranges of the second phase transition (DPPI-xP-rich domain) also differ among the various DPPI-xP lipids; the phase transition of DPPI-4P is slightly sharper than for the two other isomers and the endpoint of the transition is the highest (≈63°C). The endpoint of the DPPI-5P phase transition is found at a slightly lower temperature, whereas the phase transition of DPPI-3P is completed even below 60°C.

The presence of two transitions in the $\nu_s(CH_2)$ versus temperature plot of the respective DPPI-xP component indicates incomplete demixing, i.e., some of the DPPI-xP molecules are in a DPPC-rich environment (phase transition concurrent with DPPC-d_{62}), whereas a varying amount of DPPI-xP is sequestered into an individual domain (second broad transition). In this context it is worth noting that the infrared spectroscopic characterization of distearoylphosphatidylcholine (DSPC)/dimyristoylphosphatidylcholine (DMPC)-d_{54} mixed vesicles (Leidy et al., 2001) also furnished results consistent with gel/fluid coexisting phases of varying composition.

At first glance, the IR and DSC results appear to be in disagreement, because the high-temperature transitions of the DPPI-xP components found in the IR experiments cannot be identified in the calorimetric measurements. Even a 20-fold enhancement of the total lipid concentration (resulting in 0.9 mM of phosphoinositide) did not furnish any clear transition above 43°C in the DSC thermograms (a further concentration increase would be cost prohibitive). However, it is not uncommon that such broad transitions are elusive, particularly taking into account the low concentration of the phosphoinositide component (Leidy et al., 2001). This implies that the phase transition peak found in the DSC thermograms represents in the majority the DPPC component and should be compared to the IR data acquired for DPPC-d_{62}. Although the phase transition temperatures from the two types of measurements cannot be directly compared (the isotopic labeling of DPPC results in a T_m shift), the width of the transition and the relative temperature shift of the phase transition should be comparable (though it should

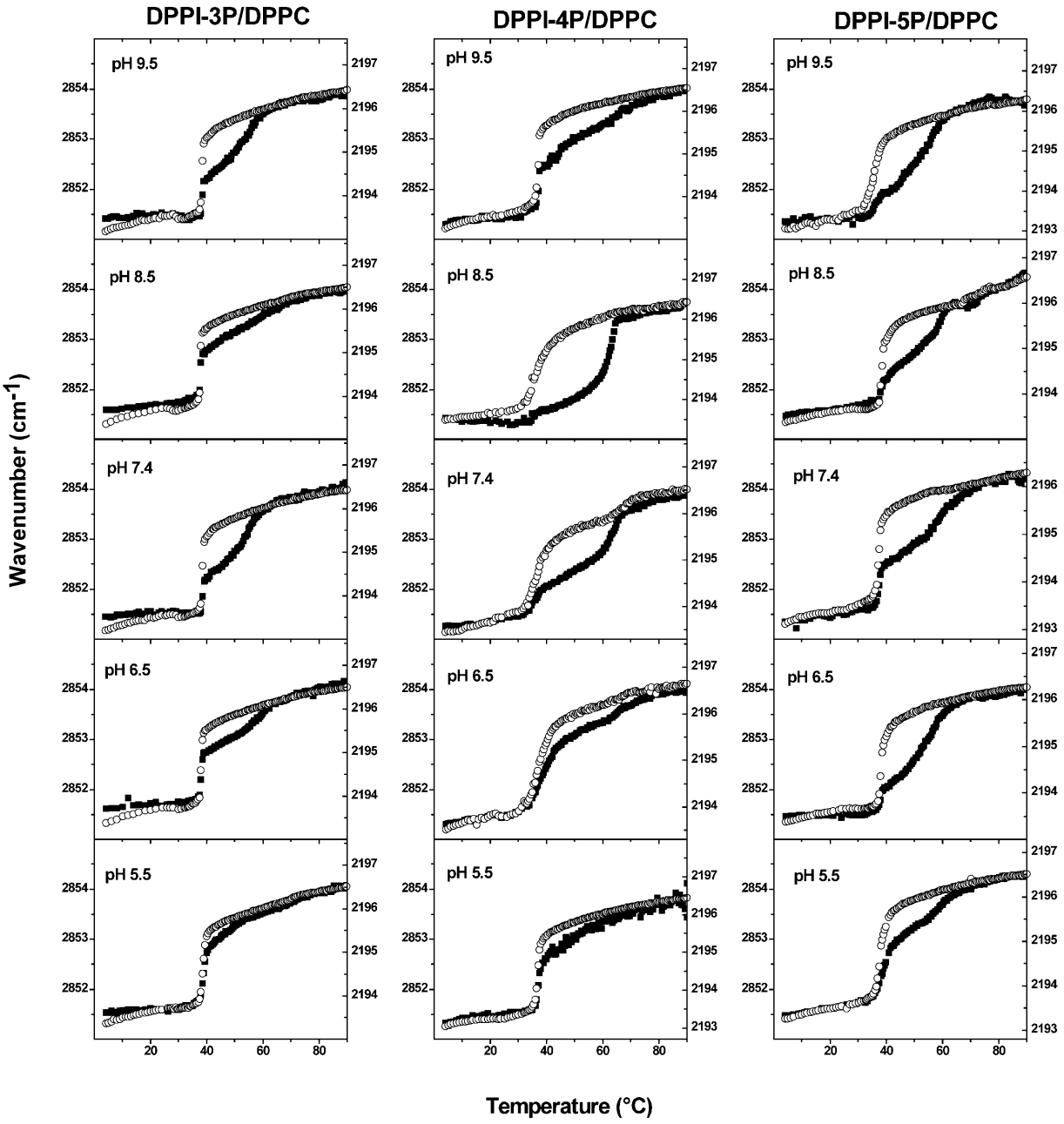

FIGURE 4 Methylene stretching band frequencies versus temperature for DPPC-d_{62}/DPPI-xP (85:15) mixed multilamellar vesicles. (■) $\nu_s(CH_2)$ of DPPI-xP (*left axis*); (○) $\nu_a(CD_2)$ of DPPC-d_{62} (*right axis*). Total experiment time = 30 h. Total lipid concentration = 40.6 mM. Buffer = 100 mM NaCl, 10 mM buffer, 0.1 mM EDTA.

be noted that the phase transition of pure DPPC-d_{62} vesicles is slightly broadened in comparison to proteated DPPC). The DSC thermograms of the DPPC/DPPI-3P mixed vesicles are characterized by a narrow transition peak, which shifts from 41.6°C to 40.5°C as the pH value is increased (Fig. 3). Similarly, the IR data reveal a quite narrow transition of the DPPC-d_{62} component and a shift to lower temperatures as the pH is decreased. For DPPC/DPPI-4P narrow DSC peaks are found for pH 5.5 and 9.5, respectively, and broadened peaks for pH 6.5–8.5. This is also reflected in the corresponding IR data, which show for pH 6.5–8.5 an extended transition region for the DPPC-d_{62} phase transition and a shift to lower temperatures.

In the course of our experiments it turned out that the reproducibility of the relative magnitude of the two transitions was dependent on an accurate control of the sample preparation conditions (each experiment was repeated at least three times). The time the multilamellar vesicles were tempered at high temperature before the IR experiment was started was a particularly important factor. If this curing time

was too short, the DPPI-xP component entered the phase transition concurrent with DPPC-d_{62}; however, after completion of ≈30% of the phase transition, lipid demixing occurred and the phosphoinositide methylene stretching band frequencies dropped to a significantly lower value (indicating an improved acyl chain order). Subsequently, the DPPI-xP component entered the broad high-temperature transition, whereas the DPPC-d_{62} phase transition behavior appeared to be largely unaffected by the apparent demixing event. Such a sudden reduction of the methylene stretching band frequencies throughout the phase transition was also observed for DSPC in DMPC-d_{54}/DSPC mixed vesicles (Leidy et al. 2001) and was attributed to dynamic demixing in the phase transition.

The IR results show that in the temperature range between ~40 and 60°C, phosphatidylinositol monophosphate-enriched gel-phase domains are present within a fluid DPPC-d_{62}-rich surrounding phase. The formation of these ordered domains appears to be highly pH-dependent and the gel/liquid-crystalline phase transition temperatures of the DPPI-xP-rich domains are significantly higher than those found for DPPI vesicles. These two observations indicate that the respective phosphomonoester group contributes significantly to the stability of the phosphoinositide-rich domain. Furthermore, the position of the phosphomonoester group at the inositol ring appears to influence the magnitude of this stabilization because the phase transition temperatures of DPPI-4P-rich domains are markedly higher than the corresponding values of the DPPI-3P-rich domains.

Physiological phosphoinositide concentrations are well below the 15% phosphoinositide concentration used for the IR experiments described above. To test whether the observed formation of phosphoinositide-enriched domains is caused by these quite high concentrations, we repeated the IR experiments for the DPPC-d_{62}/DPPI-4P mixture at pH 7.4 for 10%, 5%, and 3% DPPI-4P (Fig. 5). The high-temperature transition of the phosphoinositide component is clearly visible, while the low-temperature transition shrinks as the DPPI-4P content is being lowered. Even for 1% DPPI-4P, the high-temperature transition was still discernable, though the scatter of the data becomes quite pronounced due to a poor signal/noise ratio (not shown). As expected, the reduction of the DPPI-4P concentration increases the cooperativity of the DPPC-d_{62} gel/liquid-crystalline phase transition and moves the phase transition close to the temperature found for pure DPPC-d_{62}. These results indicate that a relative reduction of the DPPI-4P concentration is accompanied by a more complete demixing of the two lipid components.

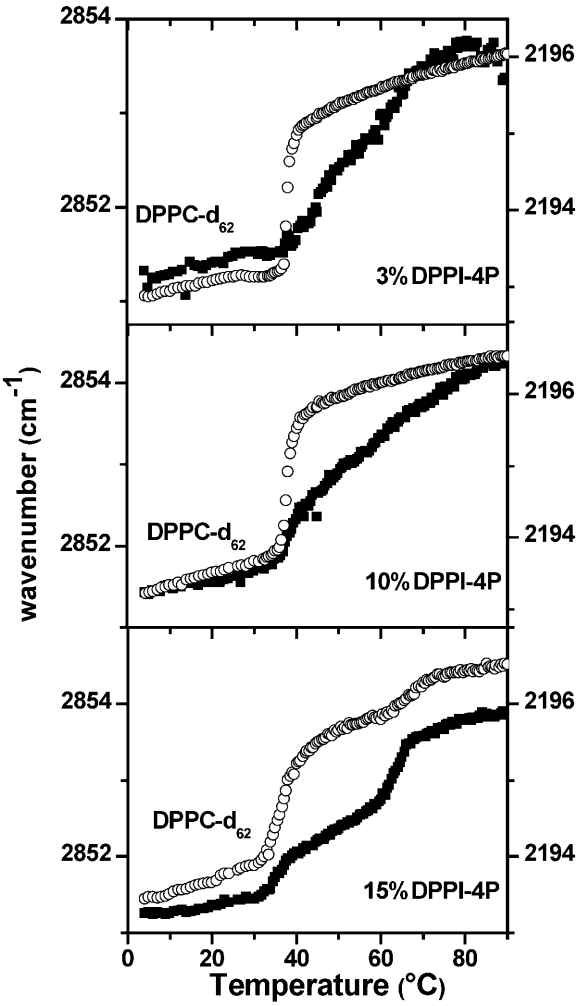

FIGURE 5 Methylene stretching band frequencies versus temperature for DPPC-d_{62}/DPPI-4P mixed multilamellar vesicles for 15%, 10%, and 3% DPPI-4P concentration. (■) $\nu_s(CH_2)$ of DPPI-4P (*left axis*); (○) $\nu_a(CD_2)$ of DPPC-d_{62} (*right axis*). Total experiment time = 30 h. Total lipid concentration = 40.6 mM. Buffer = pH 7.4, 100 mM NaCl, 10 mM HEPES, 0.1 mM EDTA.

Fluorescence resonance energy transfer measurements

Fluorescence quenching and resonance energy transfer methods have been widely used to study microdomain formation in biological model membrane systems (London, 2002). Both techniques usually rely on the preferential enrichment of the respective fluorescently labeled molecules in either the ordered microdomains or the disordered ambient phase. In the case of FRET measurements, co-localization of the two fluorophores results in maximum energy transfer, while the opposite is observed when the two labeled molecules partition into different phases. This differential enrichment is usually achieved by using probe molecules with different spatial requirements, e.g., *N*-(lissamine™-rhodamine B)-dimyristoylphosphatidylethanolamine (Rh-DMPE)/NBD-DMPE (Leidy et al., 2001; Loura et al., 2001; Stillwell et al., 2000) or DiO-C18:1/DiI-C20:0 (Feigenson and Buboltz, 2001). The aforementioned measurements were aimed at the characterization of acyl chain-induced lipid partitioning, whereas this study is concerned with the characterization of headgroup-driven microdomain formation.

Therefore, a different experimental strategy was employed by using acyl chain-labeled lipid molecules with headgroups matching the two components of the respective binary lipid mixture. From the point of view of chain composition, both labeled lipid molecules prefer to enrich in the most fluid phase. These preferences are expected to be altered by strong interactions in the headgroup moiety, which should result in co-localization of headgroup-matched unlabeled and labeled lipid molecules. Such a behavior would increase the distance between the two types of labeled lipid molecules and, therefore, a reduction of the resonance energy transfer should occur. To avoid *trans* bilayer energy transfer and to enable pH titration, the labeled lipids were fused into the outer leaflet of the bilayer by adding them as aqueous dispersions to the preformed unilamellar mixed vesicles. All experiments were carried out at 70°C, i.e., well above the gel/liquid-crystalline phase transition of all investigated mixtures. In all cases, we used NBD as the donor and BODIPY as the acceptor fluorophores (see Materials and Methods).

To test the validity of the described experimental approach, three systems of known mixing behavior were investigated (Fig. 6). For a phosphatidylcholine-only system, DPPC/NBD-PC/BODIPY-PC, a pronounced energy transfer was found (high acceptor/donor emission ratio), which indicates that the amount of labeled lipids inserted into the vesicles is sufficient for energy transfer to occur. The energy transfer increases slightly as the pH is being decreased. It is important to note that a solution of the two labeled lipids alone showed no NBD and only a minute BODIPY emission (in contrast to NBD, BODIPY is fluorescent in an aqueous environment and the small emission intensity is due to minor direct excitation of the fluorophore). To test whether the experimental protocol is suitable for the identification of pH-dependent microdomain formation, we investigated DPPC/dipalmitoylphosphatidylglycerol (DPPG) and DPPC/DPPA (both 85:15) mixtures in the liquid-crystalline phase (T = 70°C). For both systems, the mixing properties in the liquid-crystalline phase have been investigated by Blume and co-workers, who found, based upon calorimetric measurements, that DPPC and DPPG mix almost ideally at pH 7, whereas at pH 2 a more or less pronounced clustering of like molecules occurs (Garidel et al., 1997b). For the DPPC/DPPA mixture they observed preferred DPPC/DPPA interaction at pH 7 and demixing at about pH 4 (Garidel et al., 1997a). The FRET data presented in Fig. 6 *B* are largely in agreement with these findings (Fig. 6 *A* shows the fluorescence emission spectra for the respective mixture at pH ≈7.4). For the DPPG/DPPC mixture (labeled with NBD-PG/BODIPY-PC), a high energy transfer is observed for pH values between 3 and 10, while the acceptor/donor ratio is slightly diminished for pH 2. The DPPA/DPPC system (NBD-PA/BODIPY-PC) exhibits an enhanced transfer ratio at pH 8–10, whereas toward lower pH values an increasingly pronounced lipid demixing is observed (characterized by a lower transfer ratio). Considering the low ionic strength utilized in the experiments by Blume and co-workers (which results in lipid demixing at higher pH values than for higher ionic strengths (Garidel et al., 1997a)), the DPPC/DPPA mixing properties derived from the FRET data agree well with the respective mixing properties obtained from the calorimetric measurements.

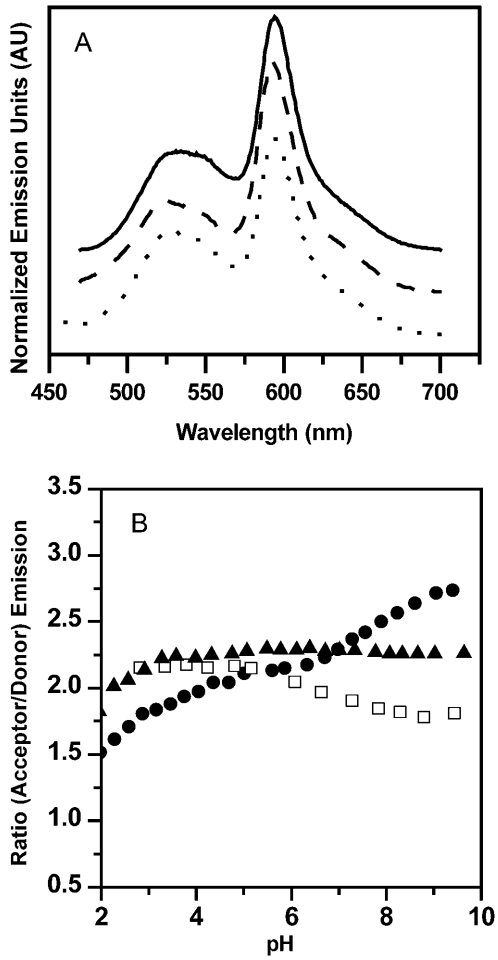

FIGURE 6 (*A*) Fluorescence spectra for various lipid mixtures at pH ≈7.4 (70°C, total lipid concentration = 0.3 mM). (*Dotted line*) DPPC labeled with NBD-PC (0.6 mol %) and BODIPY-PC (0.7 mol %); (*dashed line*) DPPC/DPPA (85:15) labeled with NBD-PA (0.6 mol %) and BODIPY-PC (0.7 mol %); (*solid line*) DPPC/DPPG (85:15) labeled NBD-PG (0.6 mol %) and BODIPY-PC (0.7 mol %). Buffer = 100 mM NaCl, 10 mM HEPES, 0.1 mM EDTA. Labeled lipids were fused into the outer leaflet of the preformed unilamellar vesicles. (*B*) Corresponding ratios of the acceptor (≈591 nm) and donor (≈534 nm) emission intensities as a function of pH. (□) PC/PC; (●) PA/PC; (▲) PG/PC.

It is important to note that the partitioning of the labeled PG or PA lipid is governed by mutual headgroup interactions, whereas in the case of the labeled PC lipid the preferences are largely determined by the bulky properties of the acyl chains, i.e., the lipid prefers a disordered environment. It cannot be ruled out that small amounts of the labeled PC lipid partition into PA- or PG-rich microdomains because the order differences between these domains and the surrounding PC phase will most likely be modest. As a conse-

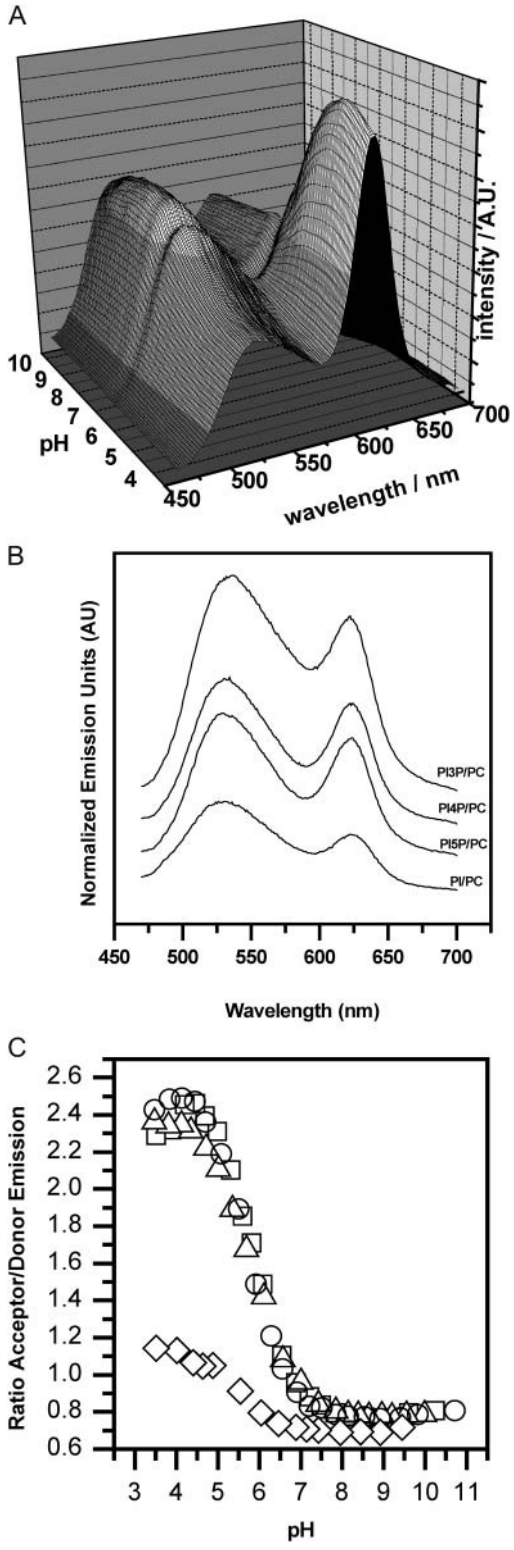

FIGURE 7 (*A*) Fluorescence spectra for DPPC/DPPI-3P (85:15) mixed vesicles labeled with 0.6 mol % NBD-PC and 0.7 mol % BODIPY-PI-3P (0.3 mM total lipid concentration, 70°C). Labeled lipids were fused into the outer leaflet of the preformed unilamellar vesicles. Lipid suspensions were titrated with 0.1 M HCl from pH 10 to 3.5 in steps of ≈0.3. Buffer = 100 mM NaCl, 10 mM HEPES, 0.1 mM EDTA. (*B*) Fluorescence spectra for DPPC/DPPI and DPPC/DPPI-xP (85:15) mixed vesicles (pH ≈7.4, total lipid concentration = 0.3 mM, 70°C). Labeled NBD-PC (0.6 mol %) and BODIPY-PI or BODIPY-PI-xP (0.7 mol %), respectively, were fused into the outer leaflet of the preformed unilamellar vesicles. (*C*) Corresponding ratios of the acceptor (≈617 nm) and donor (≈534 nm) emission intensities as a function of pH. (◇) PI/PC; (□) PI-5P/PC; (○) PI-4P/PC; (Δ) PI-3P/PC.

quence, even in cases with a pronounced lipid demixing some residual energy transfer is likely to occur and the transfer ratios will be larger than zero. However, the FRET results (see also below) show that the transfer ratio difference between the mixed and demixed lipid state is sufficient to monitor headgroup-dependent microdomain formation.

Fig. 7 *A* shows the fluorescence spectra for DPPC/DPPI-3P (85:15) labeled with NBD-PC (0.6 mol %) and BODIPY-PI-3P (0.7 mol %) as a function of pH value. It can clearly be seen that the acceptor emission intensity is low at high pH and increases as the pH is lowered, i.e., at high pH DPPI-3P-rich microdomains are apparently formed. Fig. 7 *B* displays the fluorescence spectra for the DPPC/DPPI and DPPC/DPPI-xP mixtures at pH ≈7.4, whereas Fig. 7 *C* shows the acceptor/donor emission ratios for mixed vesicles composed of DPPC and DPPI, DPPI-3P, DPPI-4P, or DPPI-5P (85:15; all samples were labeled with NBD-PC and BODIPY-PI or BODIPY-PIxP; $x = 3$, 4, or 5).

For the DPPC/DPPI vesicles, the transfer ratio increases from ≈0.7 (pH >6.5) to ≈1.1 (midpoint of the transition pH ≈5.4). The observed fluorescence intensities in the raw spectra showed a typical magnitude (Fig. 7 *B*), which indicates that the labeled lipids inserted well into the preformed vesicles and therefore, the low transfer ratios indicate pronounced demixing at pH values >6.5. Although at lower pH the lipids appear to be slightly better mixed (higher transfer ratio), it is important to note that the transfer ratio is still characteristic of a largely demixed state.

For all DPPC/DPPI-xP mixtures, the acceptor/donor emission ratios are small for high pH values, while at low pH the ratios are significantly enhanced. The transition from the demixed (low ratio) to the mixed state (high ratio) occurs between pH ≈7.2 and ≈4.8 (midpoint pH ≈5.9–6.0) and was found to be fully reversible. The midpoint of this transition appears to be largely independent of the position of the phosphomonoester group at the inositol ring (i.e., for all DPPI-xP isomers the same pH dependence was found). In comparison to the DPPC/DPPI mixed vesicles, the midpoint is found at slightly higher pH values (pH 5.9 vs. pH 5.4) and, most importantly, the acceptor/donor emission ratios at low pH are significantly higher for the DPPC/DPPI-xP mixtures. In fact, the ratios are comparable to those observed for the single-component phosphatidylcholine vesicles (see Fig. 6 *B*), which implies that the DPPC and DPPI-xP lipids are mixed at low pH. It is important to stress that all experiments were carried out at 70°C, i.e., the lipid mixtures were in the liquid-crystalline state and the observed microdomain formation can be attributed to a fluid/fluid demixing event.

Although the above experiments were conducted at a temperature which is commensurate with a fluid lipid state, the saturated chains of the lipid molecules might still aid the formation of phosphoinositide-enriched microdomains. To test whether fluid/fluid demixing also occurs for PC/PI-xP mixtures with natural chain compositions, we repeated the above experiments with POPC/brain PI and POPC/brain PI-4P mixtures (the brain PI and PI-4P acyl chain composition is characterized by a high degree of unsaturation). In both cases, the data agree well with the corresponding results for the lipids with saturated chains (Fig. 8). This implies that natural chain PI-4P forms at physiological pH microdomains, which apparently disintegrate as the pH level is being lowered. Presently, PI-3P and PI-5P are not commercially available with natural chain composition, but based upon the results presented for the saturated chain analogs, it is very likely that natural chain PI-3P and PI-5P also form microdomains at pH >7.

As noted above, physiological phosphoinositide concentrations are considerably lower than the concentrations used for the described FRET experiments. To test whether lower phosphoinositide percentages also furnish microdomain formation at high pH values, we investigated the POPC/brain PI-4P system with 10%, 5%, and 2% phosphoinositide content (not shown). In all cases, we observed the same pH dependence of the transfer ratios as found for 15% phosphoinositide content. However, the validity of the experiments with 2% PI-4P concentration is limited because the ratio of labeled/unlabeled PI-4P becomes almost 1:1 (to achieve a sufficient energy transfer in the completely mixed state, the amount of labeled PI-4P had to be fixed at 0.7 mol % total lipid).

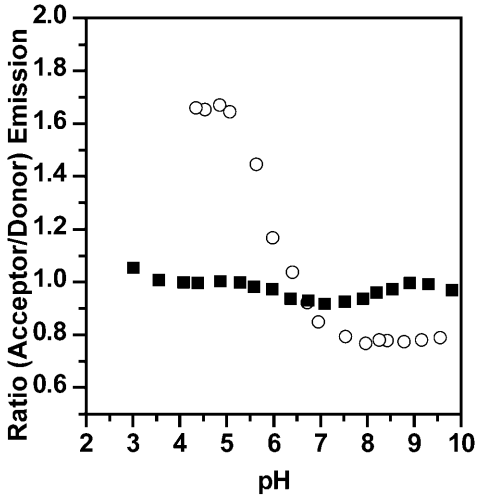

FIGURE 8 Ratios of the acceptor (≈617 nm) and donor (≈534 nm) emission intensities as a function of pH for brain POPC/PI and brain POPC/PI-4P (85:15), respectively (total lipid concentration = 0.3 mM, 20°C). Labeled NBD-PC (0.6 mol %) and BODIPY-PI or BODIPY-PI-4P (0.7 mol %), respectively, were fused into the outer leaflet of the preformed unilamellar vesicles. (■) PI/PC; (○) PI-4P/PC.

DISCUSSION

Phosphatidylcholine/phosphatidylinositol mixed vesicles

The FRET experiments revealed for pH values >6 a distinct formation of DPPI-enriched microdomains, which appears to be slightly altered for smaller pH values. For PI lipids with unsaturated chains, PC/PI demixing is clearly observed and the pH dependence is even less pronounced than for the corresponding case with the saturated acyl chains. The DSC experiments provided novel information about the DPPI phase behavior; however, due to the similar DPPI and DPPC phase transition temperatures, the mixing behavior of these two lipids cannot be investigated by DSC.

It is interesting to compare the results obtained for PI to those for PG, because both molecules have a phosphodiester as well as hydroxyl groups. For PG, the FRET data are consistent with a mixed PC/PG phase at high pH, while below pH 3 demixing occurs. Blume and co-workers (Garidel et al., 1997b) found a similar behavior in their calorimetric measurements and argued that at high pH PC/PG complexes are being formed due to charge repulsion between PG headgroups. At low pH, the phosphodiester group becomes partly protonated and hydrogen bond formation between adjacent phosphodiester groups becomes feasible and therefore, an enhanced mutual PG interaction (resulting in PC/PG demixing) is observed. In the case of PI, the repulsive effect of the phosphodiester group at high pH is apparently overcome by intermolecular hydrogen bond formation between adjacent hydroxyl groups and/or between the phosphodiester and hydroxyl groups. This observation sets phosphatidylinositol apart from phosphatidylglycerol, where the involvement of the hydroxyl groups in the mutual interaction is minor (most likely due to an unfavorable steric arrangement).

The FRET transfer ratios are indicative of a largely demixed PC/PI state for all pH values. However, the slight pH dependence of the mutual PI interaction is unexpected and cannot be attributed to an increased protonation of the phosphodiester group (the respective pK_a value is ~2.5–3; Abramson et al., 1968). Instead, the increased proton concentration apparently affects the electrostatic environment of the inositol ring, which might cause a change in the protonation pattern of the inositol ring hydroxyl groups and as a consequence, a slightly reduced intermolecular hydrogen bond formation. In this context it is worth mentioning that infrared studies by Carrier and Wong (1996) highlight the importance of the inositol ring hydroxyl groups as well as headgroup bound water molecules for the mutual phosphatidylinositol interaction.

Phosphatidylcholine/phosphatidylinositol monophosphate mixed vesicles

The experiments presented above were designed to investigate the pH-dependent formation of phosphatidylinositol

monophosphate-enriched microdomains. The IR transmission measurements investigated the pH-dependent stabilization of phosphatidylinositol monophosphate-enriched gel phases, whereas the FRET experiments explored the pH-dependent fluid/fluid demixing of PC/PI-xP mixed vesicles. The results from both techniques clearly support the notion of a pH-dependent PC/PI-xP demixing, which is most pronounced for pH 7–9.5. Based upon the pK_{a2} of micellar PI-4P (6.3; van Paridon et al., 1986), it can be assumed that the phosphomonoester groups of the respective PI-xP are largely deprotonated (double-negatively charged) for the pH range where the strongest mutual interaction is found. In this context it is worth mentioning that the respective pK_{a2} values will be influenced by the position of the phosphomonoester group at the inositol ring. For micellar PI-4,5-P_2, the 4′ position exhibited a pK_{a2} value of 6.7, whereas for the 5′ position the pK_{a2} equaled 7.6 (van Paridon et al., 1986). Similar dependencies of the pKa_2 values were found for inositol phosphates (Schlewer et al., 1999). Although these pKa_2 variations are expected to modulate slightly the mutual phosphatidylinositol monophosphate interaction, it can be safely assumed that at high pH (pH 8–9) the phosphomonoester group is largely deprotonated for all PI-xP derivatives.

The increased mutual interaction of phosphatidylinositol monophosphates above the pK_{a2} of the respective phosphomonoester group is in contrast to the results obtained for phosphatidic acid, where a stabilization of the gel phase was found between the pK_{a1} and pK_{a2} of the phosphomonoester group (Eibl, 1983). In this case, the enhanced gel-phase stability was attributed to the formation of a hydrogen bond network between adjacent phosphomonoester groups (Eibl, 1983), i.e., the phosphomonoester group functions as a hydrogen donor and acceptor. In the case of phosphatidylinositol monophosphates the mutual interaction is maximized for a largely deprotonated phosphomonoester group, i.e., the phosphomonoester group cannot donate a hydrogen atom for the potential formation of a hydrogen bond network and an interaction between phosphomonoester groups of adjacent molecules can be ruled out as a stabilizing factor of PI-xP-enriched domains. Furthermore, the high headgroup (≈ -3) charge should result in strong repulsive forces between the PI-xP headgroups and in contrast to what is observed, a mixed PC/PI-xP state should be favored. This unfavorable interaction is apparently overcome by hydroxyl group as well as hydroxyl/phosphodiester group interactions. Furthermore, the results obtained by IR spectroscopy indicate a stronger gel-phase stabilization (higher melting temperature) for PI-xP than for PI, which implies that phosphomonoester/hydroxyl group interactions provide additional stability to PI-xP-enriched microdomains.

For pH <5, the PI-xP phosphomonoester groups are partially protonated and the charge repulsion is generally expected to be reduced, which should lead to a stronger PI-xP mutual interaction and a more pronounced PC/PI-xP demixing. However, the data presented in this study clearly suggest the opposite, i.e., at low pH the mutual PI-xP interaction is diminished and considering the strong FRET transfer one might even suggest that PI-xP repulsive forces are dominating (which would result in PC/PI-xP mixing due to a favored interaction between unlike molecules). Presently the reasons for this behavior can only be speculated about, but it appears that the increased interfacial proton concentration reduces the ability of the inositol ring hydroxyl groups to participate in intermolecular hydrogen bond formation. In addition, hydrogen bond formation between adjacent phosphomonoester groups, as postulated for phosphatidic acid, is even for appropriate pH values (around pH 4) not a contributing factor for the mutual PI-xP interaction. Such an interaction would most certainly result in the formation of PI-xP-rich domains, which can be ruled out for pH values <5 based upon the IR and FRET measurements. Apparently, it is unfavorable for phosphatidylinositol monophosphates to adopt an inositol ring orientation that enables hydrogen bond formation between adjacent phosphomonoester groups.

This study was partly driven by the hypothesis that the position of the phosphate group at the inositol ring is a crucial factor for the mutual interaction of phosphatidylinositol monophosphates. The FRET results did not furnish results in support of this hypothesis because all three investigated PI-xP lipids showed a similar pH-dependent mixing behavior with phosphatidylcholine. However, the IR experiments revealed significant differences in the stability of the PI-xP-rich gel phase. This stabilization was most pronounced for DPPC/DPPI-4P mixed vesicles, which showed at pH 8.5 (Fig. 5) the most complete demixing and the highest phase transition temperature for the DPPI-xP component (endpoint of the phase transition $\approx$63°C). In contrast, DPPC/DPPI-3P mixed vesicles exhibited a narrower DSC peak (Fig. 3), the IR experiments revealed a less pronounced separation of the DPPC-d_{62} and DPPI-3P phase transitions, and the endpoint of the DPPI-3P phase transition ($\approx$58°C) was lower than for DPPI-4P. The corresponding measurements for the DPPC/DPPI-5P mixtures showed with respect to DPPI-3P a larger, and in comparison to DPPI-4P, a reduced gel-phase stability. It is tempting to speculate that the relative gel-phase stability (DPPI-4P $>$ DPPI-5P $>$ DPPI-3P) manifests itself also in the stability of fluid PI-xP-rich microdomains. Considering that the pH dependence of the DPPC/DPPI-xP gel-phase miscibility was paralleled by the pH dependence of the fluid/fluid PC/PI-xP demixing, it appears to be likely that the stability of the fluid PI-xP microdomains follows the same order, i.e., PI-4P $>$ PI-5P $>$ PI-3P. Although it bears some risks to compare absolute methylene stretching band frequencies between different lipid systems, it is worth noting that the $\nu_s(CH_2)$ band frequencies for DPPI-4P in the fluid state ($>$63°C) are lower than the corresponding values for DPPI-3P and DPPI-5P (see Fig. 4, pH 8.5), which is in general agreement with the above-postulated stability differences of PI-xP domains.

In recent years, sphingolipid- and cholesterol-enriched microdomains (rafts) have received considerable attention because of their apparent involvement in a variety of important signaling processes. The formation of such rafts is driven by interactions in the hydrophobic moiety, i.e., due to the presence of cholesterol, solid-phase sphingolipid domains are transformed into liquid-ordered domains. In contrast to this chain-driven event, phosphatidylinositol monophosphate microdomain formation is a headgroup dominated process and the presence of cholesterol might aid but is not required for the domain formation. For the description of PI-xP-rich domains in the fluid state (i.e., DPPC/DPPI-xP mixtures at high temperatures or natural chain PI-4P/POPC), the term ''liquid-ordered domain'' was intentionally avoided because the structural and morphological properties of these domains are largely unknown. However, hydrogen bond formation between adjacent PI-xP headgroups is expected to result in a decreased lateral mobility and, therefore, an enhanced positional order.

The preferential enrichment of phosphatidylinositol monophosphates in organized domains has been highlighted as a key factor for a variety of physiological functions (Miaczynska and Zerial, 2002) and the results presented above suggest that mutual phosphatidylinositol monophosphate interaction might be an important aspect for in vivo domain formation. For example, it has been shown that a considerable part of the phosphoinositide pool in erythrocytes is metabolically inaccessible to phosphoinositide-specific phosphatases and kinases (King et al., 1987; Müller et al., 1986). Müller et al. (1996) studied the effect of intracellular pH on the turnover of PI-4P phosphomonoester groups and found for pH 6.7 that ≈70% of the PI-4P pool was enzyme accessible, whereas at pH 7.8 this value dropped to ≈40%. It appears to be likely that this reduction in enzyme accessible PI-4P is a reflection of an increased domain formation at pH 7.8, which would be consistent with the enhanced mutual interaction of PI-4P found for that pH range in this study. Phosphatidylinositol-3-phosphate has been identified as a key domain organizer in the endocytic pathway (Miaczynska and Zerial, 2002), which is characterized by progressive lowering of the luminal pH. Although PI-3P is initially not exposed to the low luminal pH in late endosomes, the reduced mutual PI-3P interaction might be of relevance for subsequent degradation processes of the internal membranes of this multivesicular organelle (Kobayashi et al., 2002).

CONCLUSIONS

This study provides evidence that the mutual interaction of phosphatidylinositol monophosphates is pH-dependent and between pH ≈7 and ≈9.5 results in the formation of PI-xP-enriched microdomains. The formation of these microdomains was observed for lipid mixtures in the gel phase as well as for natural chain lipids in the fluid phase. The PI-xP-enriched microdomains are presumably stabilized by a hydrogen bond network, which utilizes the inositol ring hydroxyl groups as hydrogen donors, while the phosphomonoester, -diester, and accessible hydroxyl groups in adjacent molecules function as acceptors. An important aspect of the mutual phosphatidylinositol monophosphate interaction is its apparent weakening for slightly acidic pH levels (pH ≈4), which results in the disintegration of phosphatidylinositol monophosphate-enriched microdomains. While the pH dependence of the mutual phosphatidylinositol monophosphate interaction was largely the same for all investigated phosphatidylinositol monophosphates, it turned out that the relative stability of PI-xP-enriched microdomains (pH 7–9.5) was governed by the position of the phosphomonoester group at the inositol ring (PI-4P > PI-5P > PI-3P).

The results presented in this article highlight the importance of headgroup interactions for lipid microdomain formation. Experiments in cellular systems will be needed to judge how much the observed mutual interaction contributes to the in vivo stabilization of phosphatidylinositol monophosphate-enriched microdomains, but obviously such interactions are potentially an important aspect for phosphoinositide mediated protein functions which deserve increased attention.

The help of Andrea N. Todaro and Stephan M. Woods in acquiring some of the FRET data is gratefully acknowledged.

This research was funded by grants from the National Institutes of Health (R01-AR-038910-15) and the Ohio Board of Regents.

REFERENCES

Abramson, M. B., G. Colacicco, R. Curci, and M. M. Rapport. 1968. Ionic properties of acidic lipids. Phosphatidylinositol. *Biochemistry.* 7:1692–1698.

Bodin, S., S. Giuriato, J. Ragab, B. M. Humbel, C. Viala, C. Vieu, H. Chap, and B. Payrastre. 2001. Production of phosphatidylinositol 3,4,5-trisphosphate and phosphatidic acid in platelet rafts: evidence for a critical role of cholesterol-enriched domains in human platelet activation. *Biochemistry.* 40:15290–15299.

Botelho, R. J., M. Teruel, R. Dierckman, R. Anderson, A. Wells, J. D. York, T. Meyer, and S. Grinstein. 2000. Localized biphasic changes in phosphatidylinositol-4,5- bisphosphate at sites of phagocytosis. *J. Cell Biol.* 151:1353–1367.

Caroni, P. 2001. Actin cytoskeleton regulation through modulation of PI(4,5)P-2 rafts. *EMBO J.* 20:4332–4336.

Carricaburu, V., K. A. Lamia, E. Lo, L. Favereaux, B. Payrastre, L. C. Cantley, and L. E. Rameh. 2003. The phosphatidylinositol (PI)-5-phosphate 4-kinase type II enzyme controls insulin signaling by regulating PI-3,4,5- trisphosphate degradation. *Proc. Natl. Acad. Sci. USA.* 100:9867–9872.

Carrier, D., and P. T. T. Wong. 1996. Effect of dehydration and hydrostatic pressure on phosphatidylinositol bilayers: an infrared spectroscopic study. *Chem. Phys. Lipids.* 83:141–152.

Eibl, H. 1983. The effect of the proton and of monovalent cations on membrane fluidity. *In* Membrane Fluidity in Biology. R. C. Aloia, editor. Academic Press, New York. 217–236.

Feigenson, G. W., and J. T. Buboltz. 2001. Ternary phase diagram of dipalmitoyl-PC/dilauroyl- PC/cholesterol: nanoscopic domain formation driven by cholesterol. *Biophys. J.* 80:2775–2788.

Garidel, P., C. Johann, and A. Blume. 1997a. Nonideal mixing and phase separation in phosphatidylcholine phosphatidic acid mixtures as a function of acyl chain length and pH. *Biophys. J.* 72:2196–2210.

Garidel, P., C. Johann, L. Mennicke, and A. Blume. 1997b. The mixing behavior of pseudobinary phosphatidylcholine phosphatidylglycerol mixtures as a function of pH and chain length. *Eur. Biophys. J. Biophys. Lett.* 26:447–459.

Hanbro, P. M., S. J. Byard, R. J. Bushby, P. J. H. Turnbull, N. Boden, M. Saunders, R. Novelli, and D. G. Reid. 1992. The conformational behavior of phosphatidylinositol in model membranes: ^{2}H-NMR studies. *Biochim. Biophys. Acta.* 1112:187–196.

Heimburg, T. 2000. A model for the lipid pretransition: coupling of ripple formation with the chain-melting transition. *Biophys. J.* 78:1154–1165.

Hill, M. M., J. H. Feng, and B. A. Hemmings. 2002. Identification of a plasma membrane raft-associated PKB Ser^{473} kinase activity that is distinct from ILK and PDK1. *Curr. Biol.* 12:1251–1255.

Kanaho, Y., and T. Suzuki. 2002. Phosphoinositide kinases as enzymes that produce versatile signaling lipids, phosphoinositides. *J. Biochem.* 131:503–509.

King, C. E., L. R. Stephens, P. T. Hawkins, G. R. Guy, and R. H. Michell. 1987. Multiple metabolic pools of phosphoinositides and phosphatidate in human erythrocytes incubated in a medium that permits rapid transmembrane exchange of phosphate. *Biochem. J.* 244:209–217.

Kobayashi, T., M. H. Beuchat, J. Chevallier, A. Makino, N. Mayran, J. M. Escola, C. Lebrand, P. Cosson, and J. Gruenberg. 2002. Separation and characterization of late endosomal membrane domains. *J. Biol. Chem.* 277:32157–32164.

Koynova, R., and M. Caffrey. 1998. Phases and phase transitions of the phosphatidylcholines. *Biochim. Biophys. Acta.* 1376:91–145.

Leidy, G., W. F. Wolkers, K. Jorgensen, O. G. Mouritsen, and J. H. Crowe. 2001. Lateral organization and domain formation in a two-component lipid membrane system. *Biophys. J.* 80:1819–1828.

Lemmon, M. A. 2003. Phosphoinositide recognition domains. *Traffic.* 4:201–213.

London, E. 2002. Insights into lipid raft structure and formation from experiments in model membranes. *Curr. Opin. Struct. Biol.* 12:480–486.

Loura, L. M. S., A. Fedorov, and M. Prieto. 2001. Fluid-fluid membrane microheterogeneity: a fluorescence resonance energy transfer study. *Biophys. J.* 80:776–788.

Mansour, H., D. S. Wang, C. S. Chen, and G. Zografi. 2001. Comparison of bilayer and monolayer properties of phospholipid systems containing dipalmitoylphosphatidylglycerol and dipalmitoylphosphatidylinositol. *Langmuir.* 17:6622–6632.

Marshall, J. G., J. W. Booth, V. Stambolic, T. Mak, T. Balla, A. D. Schreiber, T. Meyer, and S. Grinstein. 2001. Restricted accumulation of phosphatidylinositol 3-kinase products in a plasmalemmal subdomain during Fcγ-receptor-mediated phagocytosis. *J. Cell Biol.* 153:1369–1380.

McElhaney, R. N., and R. N. A. H. Lewis. 1995. Fourier transform infrared spectroscopy in the study of hydrated lipids and lipid bilayer membranes. *In* Infrared Spectroscopy of Biomolecules. H. H. Mantsch and D. Chapman, editors. Wiley, New York. 159–202.

McLaughlin, S., J. Y. Wang, A. Gambhir, and D. Murray. 2002. PIP2 and proteins: interactions, organization, and information flow. *Annu. Rev. Biophys. Biomolec. Struct.* 31:151–175.

Mendelsohn, R., and D. J. Moore. 1998. Vibrational spectroscopic studies of lipid domains in biomembranes and model systems. *Chem. Phys. Lipids.* 96:141–157.

Mendelsohn, R., and R. G. Snyder. 1996. Infrared spectroscopic determination of conformational disorder and microphase separation in phospholipid acyl chains. *In* Biological Membranes. K. M. Merz and B. Roux, editors. Birkhäuser, Boston, MA. 145–174.

Miaczynska, M., and M. Zerial. 2002. Mosaic organization of the endocytic pathway. *Exp. Cell Res.* 272:8–14.

Müller, E., H. Hegewald, K. Jaroszewicz, G. A. Cumme, H. Hoppe, and H. Frunder. 1986. Turnover of phosphomonoester groups and compartmentation of polyphosphoinositides in human erythrocytes. *Biochem. J.* 235:775–783.

Müller, E., H. Hegewald, R. Klinger, R. Wetzker, G. A. Cumme, and H. Frunder. 1996. Dependence on intracellular pH and Mg^{2+} of metabolic compartmentation of phosphoinositides in human erythrocytes. *Biol. Chem.* 377:851–856.

Padron, D., Y. J. Wang, M. Yamamoto, H. Yin, and M. G. Roth. 2003. Phosphatidylinositol phosphate 5-kinase Iβ recruits AP-2 to the plasma membrane and regulates rates of constitutive endocytosis. *J. Cell Biol.* 162:693–701.

Payrastre, B., K. Missy, S. Giuriato, S. Bodin, M. Plantavid, and M. P. Gratacap. 2001. Phosphoinositides—key players in cell signalling, in time and space. *Cell Signal.* 13:377–387.

Rozelle, A. L., L. M. Machesky, M. Yamamoto, M. H. E. Driessens, R. H. Insall, M. G. Roth, K. Luby-Phelps, G. Marriott, A. Hall, and H. L. Yin. 2000. Phosphatidylinositol 4,5-bisphosphate induces actin-based movement of raft-enriched vesicles through WASP-Arp2/3. *Curr. Biol.* 10:311–320.

Schlewer, G., P. Guedat, S. Ballereau, L. Schmitt, and B. Spiess. 1999. Inositol phosphates; inframolecular physico-chemical studies: correlation with binding properties. *In* Phosphoinositides: Chemistry, Biochemistry and Biomedical Applications. K. S. Bruzik, editor. American Chemical Society, Washington, DC. 255–270.

Simonsen, A., A. E. Wurmser, S. D. Emr, and H. Stenmark. 2001. The role of phosphoinositides in membrane transport. *Curr. Opin. Cell Biol.* 13:485–492.

Stenmark, H., and D. J. Gillooly. 2001. Intracellular trafficking and turnover of phosphatidylinositol 3-phosphate. *Semin. Cell Dev. Biol.* 12:193–199.

Stillwell, W., L. J. Jenski, M. Zerouga, and A. F. Dumaual. 2000. Detection of lipid domains in docosahexaenoic acid-rich bilayers by acyl chain-specific FRET probes. *Chem. Phys. Lipids.* 104:113–132.

Takizawa, T., Y. Nakata, A. Takahashi, M. Hirai, S. Yabuki, and K. Hayashi. 1998. Differential scanning calorimetry and ^{1}H-NMR study of aqueous dispersions of the mixtures of dipalmitoylphosphatidylcholine and phosphatidylinositol-4,5-bis(phosphate). *Thermochim. Acta.* 308:101–107.

van Paridon, P. A., B. de Kruijff, R. Ouwerkerk, and K. W. A. Wirtz. 1986. Polyphosphoinositides undergo charge neutralization in the physiological pH range: a ^{31}P-NMR study. *Biochim. Biophys. Acta.* 877:216–219.

Vanhaesebroeck, B., S. J. Leevers, K. Ahmadi, J. Timms, R. Katso, P. C. Driscoll, R. Woscholski, P. J. Parker, and M. D. Waterfield. 2001. Synthesis and function of 3-phosphorylated inositol lipids. *Annu. Rev. Biochem.* 70:535–602.

Wanaski, S. P., B. K. Ng, and M. Glaser. 2003. Caveolin scaffolding region and the membrane binding region of SRC form lateral membrane domains. *Biochemistry.* 42:42–56.

Wang, J. Y., A. Gambhir, G. Hangyas-Mihalyne, D. Murray, U. Golebiewska, and S. McLaughlin. 2002. Lateral sequestration of phosphatidylinositol 4,5-bisphosphate by the basic effector domain of myristoylated alanine-rich C-kinase substrate is due to nonspecific electrostatic interactions. *J. Biol. Chem.* 277:34401–34412.

Wang, Y. J., J. Wang, H. Q. Sun, M. Martinez, Y. X. Sun, E. Macia, T. Kirchhausen, J. P. Albanesi, M. G. Roth, and H. L. Yin. 2003. Phosphatidylinositol-4 phosphate regulates targeting of clathrin adaptor AP-1 complexes to the golgi. *Cell.* 114:299–310.

Zhang, W. Y., E. Crocker, S. McLaughlin, and S. O. Smith. 2003. Binding of peptides with basic and aromatic residues to bilayer membranes—phenylalanine in the myristoylated alanine-rich C-kinase substrate effector domain penetrates into the hydrophobic core of the bilayer. *J. Biol. Chem.* 278:21459–21466.

Zhuang, L. Y., J. Q. Lin, M. L. Lu, K. R. Solomon, and M. R. Freeman. 2002. Cholesterol-rich lipid rafts mediate AKT-regulated survival in prostate cancer cells. *Cancer Res.* 62:2227–2231.